Biochemical and Biophysical Research Communications 463 (2015) 309–314

Contents lists available at ScienceDirect

Biochemical and Biophysical Research Communications

journal homepage: www.elsevier.com/locate/ybbrc

Crystal structure of the karyopherin Kap121p bound to the extreme C-terminus of the protein phosphatase Cdc14p

Junya Kobayashi [a], Hidemi Hirano [a, b], Yoshiyuki Matsuura [a, b, *]

[a] Division of Biological Science, Graduate School of Science, Nagoya University, Japan
[b] Structural Biology Research Center, Graduate School of Science, Nagoya University, Japan

ARTICLE INFO

Article history:
Received 30 April 2015
Accepted 16 May 2015
Available online 28 May 2015

Keywords:
Karyopherin
Kap121p
NLS
Cdc14p
Nuclear import

ABSTRACT

In *Saccharomyces cerevisiae*, the protein phosphatase Cdc14p is an antagonist of mitotic cyclin-dependent kinases and is a key regulator of late mitotic events such as chromosome segregation, spindle disassembly and cytokinesis. The activity of Cdc14p is controlled by cell-cycle dependent changes in its association with its competitive inhibitor Net1p (also known as Cfi1p) in the nucleolus. For most of the cell cycle up to metaphase, Cdc14p is sequestered in the nucleolus in an inactive state. During anaphase, Cdc14p is released from Net1p, spreads into the nucleus and cytoplasm, and dephosphorylates key mitotic targets. Although regulated nucleocytoplasmic shuttling of Cdc14p has been suggested to be important for exit from mitosis, the mechanism underlying Cdc14p nuclear trafficking remains poorly understood. Here we show that the C-terminal region (residues 517–551) of Cdc14p can function as a nuclear localization signal (NLS) *in vivo* and also binds to Kap121p (also known as Pse1p), an essential nuclear import carrier in yeast, in a Gsp1p-GTP-dependent manner *in vitro*. Moreover we report a crystal structure, at 2.4 Å resolution, of Kap121p bound to the C-terminal region of Cdc14p. The structure and structure-based mutational analyses suggest that either the last five residues at the extreme C-terminus of Cdc14p (residues 547–551; Gly-Ser-Ile-Lys-Lys) or adjacent residues with similar sequence (residues 540–544; Gly-Gly-Ile-Arg-Lys) can bind to the NLS-binding site of Kap121p, with two residues (Ile in the middle and Lys at the end of the five residues) of Cdc14p making key contributions to the binding specificity. Based on comparison with other structures of Kap121p-ligand complexes, we propose "IK-NLS" as an appropriate term to refer to the Kap121p-specific NLS.

1. Introduction

In eukaryotes, successful completion of mitosis depends on temporal and spatial coordination of many mitotic processes such as chromosome segregation, spindle disassembly and cytokinesis. The regulation of mitotic exit involves inactivation of mitotic cyclin-dependent kinases (CDKs) and activation of counteracting protein phosphatases [1]. In the budding yeast *Saccharomyces cerevisiae*, the protein phosphatase Cdc14p is an antagonist of CDKs and is the key trigger of mitotic exit [2]. To regulate and couple multiple mitotic events, the localization and activity of Cdc14p is regulated by cell cycle-dependent changes in its association with the competitive inhibitor Net1p (also known as Cfi1p) of the RENT complex in the nucleolus [3,4]. For most of the cell cycle up to metaphase, Cdc14p is sequestered in the nucleolus in an inactive state, because Net1p binds to and inhibits Cdc14p activity. During anaphase, Cdc14p is released from Net1p in the nucleolus by at least two signaling networks (FEAR and MEN), and spreads into the nucleus and cytoplasm. This allows Cdc14p to dephosphorylate its substrates. Thus the function of Cdc14p relies on nuclear import and export of Cdc14p.

The budding yeast Cdc14p is composed of two domains, the N-terminal phosphatase domain (~350 amino acids) and the C-terminal domain (~200 amino acids) that has been proposed to contain the nuclear import and export signals [5,6]. The exportin Xpo1p (yeast CRM1) mediates nuclear export of Cdc14p, and the residues 353–367 of Cdc14p function as a leucine-rich nuclear export signal (NES) that directly binds to Xpo1p [5]. In contrast, less is know about the mechanism underlying nuclear import of Cdc14p. Although it has been shown that the C-terminal region (the last 100 amino acids) of Cdc14p contains a nuclear

* Corresponding author. Division of Biological Science, Graduate School of Science, Nagoya University, Nagoya 464-8602, Japan.
E-mail address: matsuura.yoshiyuki@d.mbox.nagoya-u.ac.jp (Y. Matsuura).

http://dx.doi.org/10.1016/j.bbrc.2015.05.060
0006-291X/

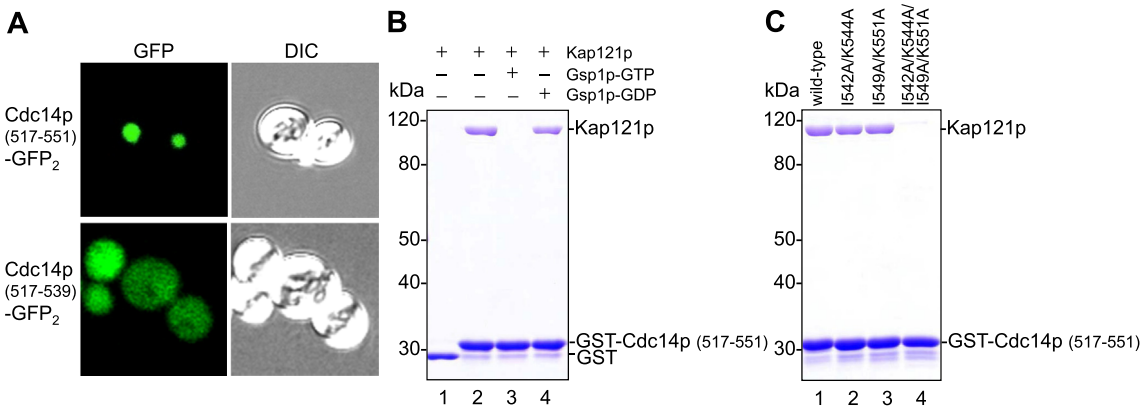

Fig. 1. Functional analyses of the C-terminal region of Cdc14p. (A) *In vivo* NLS activity assay. The localization of Cdc14p (either residues 517–551 or 517–539)-GFP-GFP fusion protein in yeast cells was monitored by GFP fluorescence. Cells were also viewed using differential interference contrast (DIC) optics. (B) GST pull-down assay. Immobilized 6 μg GST (lane 1) or 5 μg GST-Cdc14p (residues 517–551) (lanes 2-4) was incubated with either 3 μg Kap121p alone (lanes 1-2) or 3 μg Kap121p together with 10 μg Gsp1p (lane 3, Gsp1p-GTP; lane 4, Gsp1p-GDP). (C) GST pull-down assay. Immobilized 5 μg GST-Cdc14p (residues 517–551; lane 1, wild-type; lane 2, I542A/K544A mutant; lane 3, I549A/K551A mutant; lane 4, I542A/K544A/I549A/K551A mutant) was incubated with 3 μg Kap121p.

localization signal (NLS) [6], the karyopherins (nuclear import receptors) that mediate nuclear import of Cdc14p have not been identified.

Kap121p (also known as Pse1p) is an essential karyopherin that mediates nuclear import of a range of cargoes including transcription factors, ribosomal proteins, and cell-cycle regulators in the budding yeast [7]. Kap121p is a helicoidal molecule that is constructed from 24 tandem HEAT repeats, each of which consists of two antiparallel α-helices, designated A-helix and B-helix [8]. The A-helices form outer convex surface whereas the B-helices form the inner concave surface. Kap121p has a binding site for the Kap121p-specific NLS with the consensus amino acid sequence motif Lys-Val/Ile-x-Lys-$x_{1\text{-}2}$-Lys/His/Arg (where x can be any amino acid) on the inner concave surface of the central region of Kap121p (HEAT repeats 7–12) [8]. Kap121p is unique among the karyopherins in yeast in that the Kap121p-mediated nuclear import pathway is specifically inhibited during mitosis [9]. Interestingly, the period of time (in the cell cycle) when the Kap121p-specific import is inhibited is exactly the period of time when Cdc14p is released from the nucleolus and spreads to the nucleoplasm and

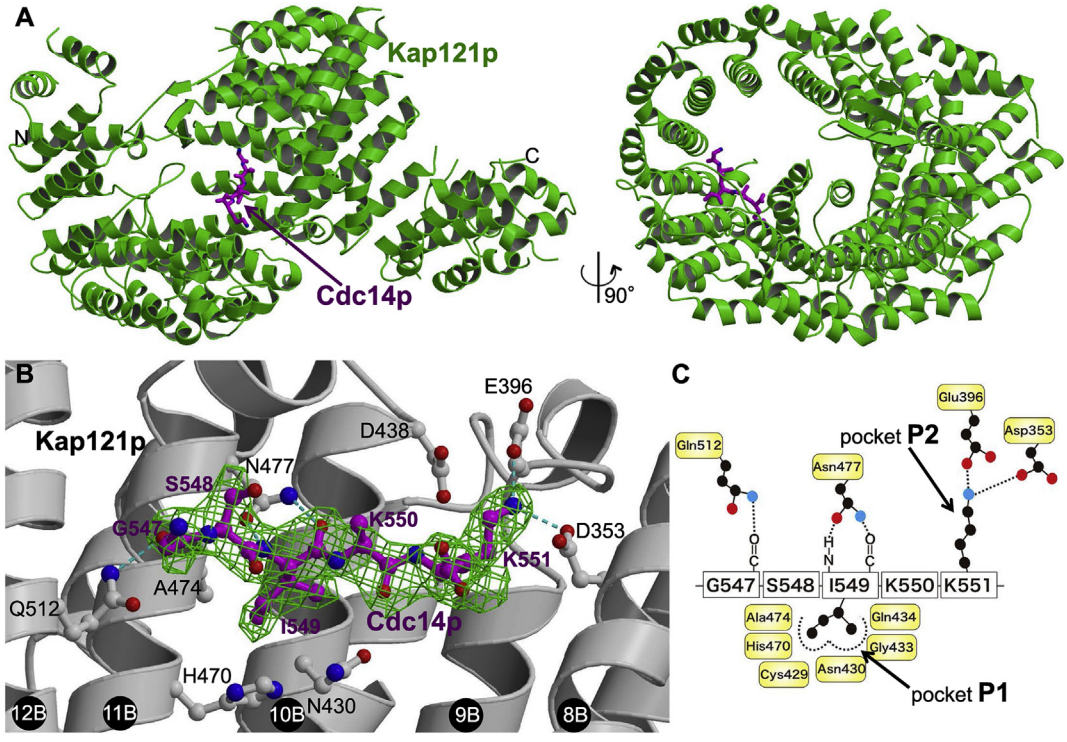

Fig. 2. Crystal structure of Kap121p-Cdc14p (residues 517–551) complex. (A) Ribbon representation of the overall structure of Kap121p (green) in complex with Cdc14p (ball-and-stick representation with magenta carbons). (B) The omit F_O–F_C electron density map (green mesh, contoured at 3σ) after refinement, with Cdc14p omitted. The density map is superposed onto the structure of Cdc14p (ball-and-stick representation with magenta carbons) bound to the NLS-binding site of Kap121p (ribbon representation in light gray). The B-helices of Kap121p HEAT repeats 8–12 that constitute the NLS-binding site are labeled 8B–12B. The dashed lines in cyan represent hydrogen bonds or salt bridges between Kap121p and Cdc14p. (C) Schematic illustration of the Kap121p-Cdc14p interactions at the NLS-binding site. Dashed lines indicate hydrogen bonds or salt bridges. (For interpretation of the references to color in this figure legend, the reader is referred to the web version of this article.)

Table 1
Crystallographic statistics.

Crystal	Kap121p (Δ80–90) bound to Cdc14p (517–551)
Data collection	
X-ray source	SPring-8 BL41XU
Wavelength (Å)	1.0
Space group	$P2_12_12_1$
Unit cell dimensions	
a, *b*, *c* (Å)	77.26, 127.76, 131.79
α, *β*, *γ* (degree)	90.0, 90.0, 90.0
Resolution range (Å)[a]	26.36–2.40 (2.47–2.40)
$R_{merge.}$ (%)[a]	10.6 (59.9)
Mean $I/\sigma(I)$[a]	7.2 (1.6)
Mean *I* half-set correlation CC(1/2)[a]	0.991 (0.753)
Completeness (%)[a]	99.5 (99.7)
Multiplicity[a]	4.3 (4.2)
No. of reflections[a]	220,860 (18,360)
No. of unique reflections[a]	51,446 (4399)
Refinement	
Resolution range (Å)	25.81–2.40
R-factor/R_{free} (%)	21.9/25.2
No. of atoms	
Protein	7808
Water	139
No. of amino acids	1022
Mean *B* factor (Å^2)	
Kap121p	66.7
Cdc14p	44.3
Water	50.9
R.m.s. deviation from ideality	
Bond lengths (Å)	0.003
Bond angles (°)	0.774
Protein geometry[b]	
Rotamer outliers (%)	0.72
Ramachandran outliers (%)	0
Ramachandran favored (%)	96.07
Cβ deviations > 0.25 Å (%)	0
Residues with bad bonds (%)	0
Residues with bad angles (%)	0
PDB code	4ZJ7

[a] Values in parentheses are for the highest resolution shell.
[b] MolProbity [17] was used to analyze the structure.

cytoplasm. We therefore hypothesized that Kap121p might be at least one of the karyopherins that mediate nuclear import of Cdc14p. In this study, we characterized the interactions between Cdc14p and Kap121p, and found that the extreme C-terminus of Cdc14p that possesses an NLS activity *in vivo* indeed binds to Kap121p in a Gsp1p-GTP-dependent manner *in vitro*. Furthermore we solved X-ray crystal structure of the Cdc14p-Kap121p complex and identified two redundant sequences at the extreme C-terminus of Cdc14p that can bind specifically to the NLS-binding site of Kap121p. We also present evidence that the Kap121p-binding sequences of Cdc14p are required for the NLS activity of the C-terminal region of Cdc14p *in vivo*.

2. Materials and methods

2.1. Protein expression and purification for biochemical assays

All proteins were expressed in the *E. coli* host strain BL21-CodonPlus(DE3)RIL (Stratagene). Glutathione *S*-transferase (GST)-Cdc14p (*S. cerevisiae*, residues 517–551) was expressed from pGEX-TEV [10], and purified over glutathione-Sepharose 4B (GE Healthcare) and gel filtration over Superdex200 (GE Healthcare). GST-Kap121p (*S. cerevisiae*, full-length) [8] was expressed from pGEX-TEV and initially purified over glutathione-Sepharose 4B (GE Healthcare). After removal of the GST tag by His-TEV protease, Kap121p was finally purified by gel filtration over Superdex200. His-Gsp1p (*S. cerevisiae*, full-length) was expressed from pET15b [11] and purified over Ni-NTA (Novagen) and by gel filtration over Superdex75 (GE Healthcare). Mutants were created using the QuickChange system (Stratagene). All DNA constructs were verified by DNA sequencing.

2.2. GST pull-down assay

Pull-down assays were performed in binding buffer (phosphate-buffered saline, 0.1% Tween-20, 0.2 mM DTT, and 0.2 mM PMSF). GST-Cdc14p was immobilized on 10 μl of packed glutathione-Sepharose 4B (GE Healthcare) beads and each binding reaction was performed by incubating the beads with reaction mixtures in a total volume of 50 μl for 1 h at 4 °C. The amounts of proteins used are indicated in the figure legends. Beads were then spun down and washed twice with 1 ml of binding buffer, and bound proteins were analyzed by SDS-PAGE and Coomassie staining.

2.3. In vivo analysis of the NLS activity

Yeast cells [*kap121Δ* cells (*MAT**a*** *his3Δ1 leu2Δ0 ura3Δ0 kap121Δ::kanMX4*) containing a wild-type *KAP121* maintenance plasmid (*CEN*, *LEU2*)] [8] were transformed with plasmids (*CEN*, *HIS3*) encoding Cdc14p (either residues 517–551 or residues 517–539)-GFP-GFP expressed from *ADH1* promoter. The localization of the Cdc14p-GFP-fusion proteins was monitored using fluorescence microscopy as described [8].

2.4. Protein expression and purification for crystallization

To prepare Kap121p-Cdc14p complex for crystallization, GST-Kap121p (Δ80-90) [8] and His/S-Cdc14p (residues 517–551) were expressed separately from pGEX-TEV and pET30a-TEV, respectively, in the *E. coli* host strain BL21-CodonPlus(DE3)RIL (Stratagene). The two sets of cells were mixed, resuspended in buffer A [30 mM Tris–HCl (pH 7.5), 150 mM NaCl, 10 mM imidazole, 7 mM 2-mercaptoethanol, and 1 mM 4-(2-Aminoethyl) benzenesulfonyl fluoride hydrochloride (AEBSF)], and lysed by sonication on ice. All subsequent purification steps were performed at 4 °C. Claryfied lysates were loaded onto Ni-NTA resin (Novagen), washed with buffer A containing 25 mM imidazole, and eluted with buffer A containing 250 mM imidazole. Tween-20 was added to the eluate to a final concentration of 0.05%. After incubating the Ni-NTA eluate with glutathione-Sepharose 4B resin (GE Healthcare), the resin was washed with buffer B [10 mM Tris–HCl (pH 7.5), 120 mM NaCl, 0.05% Tween-20, and 2 mM 2-mercaptoethanol]. The GST- and His/S-tags were cleaved off Kap121p and Cdc14p by incubating the resin overnight with His-TEV protease (0.2 mg/ml) in buffer B containing 0.2 mM AEBSF. The Kap121p-Cdc14p complex, released from the resin, was finally purified by gel filtration over Superdex200 (GE Healthcare) in buffer B without Tween-20 and the complex was concentrated to 16 mg/ml using a 3 kDa molecular weight cutoff Amicon Ultra centrifugal filter (Millipore).

2.5. Crystallization, data collection and structure determination

Crystals of Kap121p-Cdc14p complex were grown at 20 °C from 16 mg/ml protein by hanging drop vapor diffusion against 0.1 M HEPES (pH 7.0), 10% 2-propanol, and 24% PEG20000. Crystals were cryoprotected using mother liquor containing 24% PEG20000 and 10% glycerol and flash-cooled in liquid nitrogen. X-ray diffraction datasets were collected at 100 K at SPring-8 beamline BL41XU. Diffraction data were processed using MOSFLM and CCP4 programs [11]. The structure was solved by molecular replacement using

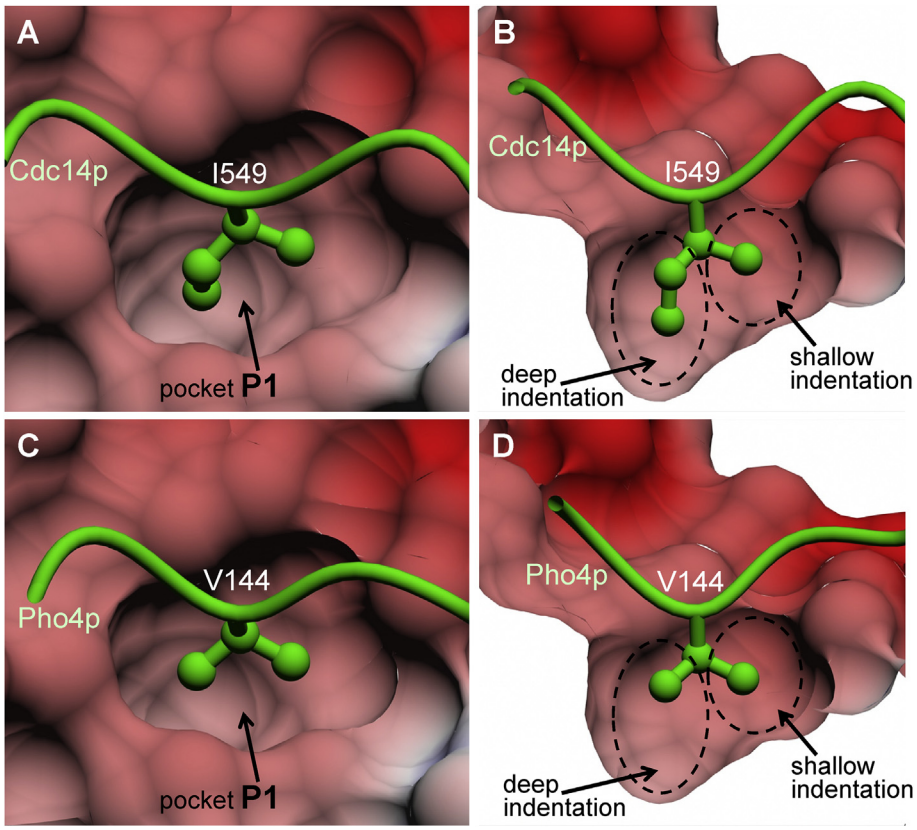

Fig. 3. The shape complementarity between the ligand sidechain and the binding pocket P1 at the NLS-binding site of Kap121p. (A, B) Structure of Kap121p-Cdc14p complex. (C, D) Structure of Kap121p-Pho4p complex (PDB code, 3W3X). Kap121p is shown in surface representation (colored by electrostatic potential: blue, positive; red, negative; white, neutral). The mainchains of Cdc14p and Pho4p are shown in worm representation (green), with the sidechain of the key hydrophobic residue (I549 of Cdc14p or V144 of Pho4p) shown in ball-and-stick representation. Shown in (B) and (D) are the transverse section of the pocket P1. (For interpretation of the references to color in this figure legend, the reader is referred to the web version of this article.)

MOLREP [12] using the structure of Kap121p-Pho4p complex (PDB code, 3W3X) [8] as a search model. The structure was refined by iterative cycles of model building using COOT [13] and refinement using REFMAC5 [14] and PHENIX [15]. TLSMD analyses [16] were used to define TLS groups for the final cycles of refinement. MolProbity [17] was used to validate the final structure. Coordinates and structure factors have been deposited in the Protein Data Bank under accession code 4ZJ7.

3. Results and discussion

3.1. The extreme C-terminus of Cdc14p that has NLS activity binds to Kap121p in a Gsp1p-GTP-dependent manner

Mohl et al. previously reported that the last 100 amino acids (residues 450–551) of Cdc14p exhibit NLS activity [6]. To examine whether residues 517–551 of Cdc14p that are rich in basic residues are sufficient for the NLS activity, we expressed Cdc14p (517–551)-GFP fusion protein in yeast cells. Fluorescence microscopy examination showed that this GFP fusion protein accumulates in the nucleus, demonstrating that the residues 517–551 of Cdc14p retain the NLS activity (Fig. 1A). To identify a candidate karyopherin that mediates nuclear import of Cdc14p, we used GST pull-down assay using purified proteins (Fig. 1B). Kap121p bound to GST-Cdc14p (residues 517–551; Fig. 1B, lane 2) but not to GST alone (Fig. 1B, lane 1), demonstrating that Kap121p binds specifically to Cdc14p (residues 517–551). We also examined whether Gsp1p (yeast Ran GTPase) competes with Cdc14p to bind Kap121p. The binding of Kap121p to Cdc14p (residues 517–551) was inhibited by Gsp1p-GTP (Fig. 1B, lane 3) but not by Gsp1p-GDP (Fig. 1B, lane 4). This suggests that Cdc14p is released from Kap121p by Gsp1p in the nucleus where Gsp1p exists primarily in the GTP-bound state but not by Gsp1p in the cytoplasm where Gsp1p exists primarily in the GDP-bound state. Taken together, the cell biological and biochemical data indicate that Kap121p can mediate nuclear import of Cdc14p and that the residues 517–551 of Cdc14p contain a Kap121p-specific NLS.

3.2. The extreme C-terminus of Cdc14p has two redundant amino acid sequences that are able to bind specifically to the NLS-binding site of Kap121p

We used X-ray crystallography to establish the precise mechanism whereby Kap121p recognizes the C-terminal region of Cdc14p. We obtained crystals of a complex formed between Cdc14p (residues 517–551) and Kap121p (Δ80-90), a functional deletion mutant of Kap121p that is suitable for crystallization [8]. The crystals diffracted X-rays to a maximal resolution of 2.4 Å, and the structure was solved by molecular replacement. After refinement, the final model of the complex (Fig. 2A) had an *R*-factor of 21.9% (R_{free} = 25.2%) and excellent geometry (Table 1). Electron density corresponding to the last five residues (^{547}GSIKK^{551}) at the extreme C-terminus of Cdc14p was identified at the NLS-biding site on the inner surface of HEAT repeats 8–12 of Kap121p (Fig. 2B), as expected from the biochemical data that Gsp1p-GTP inhibits the binding of Cdc14p to Kap121p. Although Cdc14p has an adjacent

similar sequence (^{540}GGIRK^{544}), the sidechain density for the second residue in the five Cdc14p residues visible in the omit F_O-F_C electron density map (Fig. 2B) suggested that it is more appropriate to interpret this residue as serine than to interpret this residue as glycine. We therefore built the atomic model of Cdc14p as residues 547–551, not as residues 540–544. No reliable electron density corresponding to Cdc14p was observed elsewhere on Kap121p. Kap121p recognizes Cdc14p through a network of interactions involving both mainchain and sidechain atoms of Cdc14p, as illustrated schematically in Fig. 2C. As observed in previously determined structures of Kap121p–cargo complexes [8], the Kap121p-binding residues of Cdc14p adopted an extended conformation to bind the NLS-binding site, with the mainchain of Cdc14p running in the opposite direction to that of the Kap121p HEAT repeats. The Kap121p sidechains of N477 and Q512 formed hydrogen bonds with Cdc14p mainchain and thus anchored Cdc14p mainchain on the NLS-binding site. Notably, two sidechains of Cdc14p, I549 and K551, had particularly well defined electron density (Fig. 2B) and interacted with Kap121p residues directly. The hydrophobic sidechain of I549^{Cdc14p} snugly fitted into a nonpolar pocket (hereafter designated as pocket P1) formed by Kap121p residues C429, N430, G433, Q434, H470, and A474, whereas the sidechain of K551^{Cdc14p} bound to another pocket (hereafter designated as pocket P2) and formed hydrogen bonds or salt-bridges with Kap121p residues D353 and E396. Although not within direct hydrogen-bonding distance to K551^{Cdc14p}, D438^{Kap121p} was also located close to K551^{Cdc14p} and contributed to form the acidic P2 pocket to stabilize Cdc14p binding through electrostatic interactions. The sidechain of K550^{Cdc14p} did not have well defined electron density beyond the beta carbon, and so was probably disordered. The sidechain of S548^{Cdc14p} pointed towards solvent and was not involved in interactions with Kap121p.

Although the atomic model depicted in Fig. 2B is the most plausible interpretation of the Cdc14p electron density, we cannot rule out the possibility that an adjacent similar sequence (^{540}GGIRK^{544}) in the C-terminal region of Cdc14p can also bind to the NLS-binding site of Kap121p in essentially the same way as modeled for the residues 547–551 (^{547}GSIKK^{551}), with I542 and K544 occupying the P1 and P2 pockets, respectively. This was indeed verified by mutational analyses, which also confirmed the key contributions made by the isoleucine and lysine residues of Cdc14p for the binding to Kap121p in solution (Fig. 1C). In GST pull-down assay, the double mutations I542A/K544A of Cdc14p did not appreciably decrease the binding of Cdc14p (residues 517–551) to Kap121p (see lanes 1-2 of Fig. 1C). Similarly, the double mutations I549A/K551A of Cdc14p did not appreciably affect the binding to Kap121p (Fig. 1C, lane 3). However, when these double mutations were combined, the quadruple mutations I542A/K544A/I549A/K551A decreased the binding to Kap121p to an undetectable level (Fig. 1C, lane 4). These results strongly support the idea that either of the two redundant sequences at the extreme C-terminus of Cdc14p (^{540}GGIRK^{544} and ^{547}GSIKK^{551}) is able to bind specifically to Kap121p. Consistently, deletion of residues 540–551 of Cdc14p drastically diminished the NLS activity of the C-terminal region of Cdc14p *in vivo* (Fig. 1A).

Taken together, our structural and functional analyses identified putative redundant NLS sequences (residues 540–544 and residues 547–551 of Cdc14p) that are able to bind specifically to the NLS-binding site of Kap121p. However, the possibility remains that there are other karyopherins that can mediate nuclear import of Cdc14p. The mutational analyses by Mohl et al. showed that the NLS activity of the last 100 amino acids of Cdc14p is drastically diminished by alanine substitution of R527, R528, R533, and R534 [6]. Our data reported in this study suggest that all of these arginine residues are not involved in Kap121p binding, and so it is conceivable that Cdc14p can be imported into the nucleus by multiple pathways.

3.3. Common properties of ligands that bind to the NLS-binding site of Kap121p

So far, four crystal structures of the Kap121p–ligand complexes (in which the ligand is bound to the NLS-binding site in a similar conformation) have been determined (Kap121p-Nup53p complex, Kap121p-Ste12p complex, Kap121p-Pho4p complex, and Kap121p-Cdc14p complex [8]; and this study). In all of these crystal structures, two sidechains of the ligand had well defined electron density: a hydrophobic residue (either valine or isoleucine) that fits into the P1 pocket and a lysine residue that binds to the P2 pocket at the NLS-binding site. Thus, among the conserved residues in the consensus sequence of Kap121p-specific NLS (Lys-Val/Ile-x-Lys-x_{1-2}-Lys/His/Arg, where x can be any amino acid) [8], the underlined two residues, namely valine or isoluecine that binds P1 and lysine that binds P2, appear to be particularly important as specificity determinant for the binding to the NLS-binding site of Kap121p. The P1 pocket appears to be “rigid” and does not change its shape irrespective of whether valine or isoleucine is bound to the pocket (Fig. 3). The shape of the P1 pocket is perfectly complementary to the branched sidechain of the ligand isoleucine residue, with the shorter branch of isoleucine sidechain fitting into the shallow indentation and the longer branch fitting into the deeper indentation in the P1 pocket, as observed in the structure of Kap121p-Cdc14p complex (Fig. 3A and B). When valine sidechain binds to this P1 pocket as observed in the structure of Kap121p-Pho4p complex [8], the fitting into the P1 pocket is not as intimate as observed for isoleucine, and there is a space unoccupied by the ligand sidechain at the bottom half of the deep indentation (Fig. 3C and D). Thus, the shape complementarity between isoleucine and the P1 pocket is better than that between valine and the P1 pocket. We therefore propose “IK-NLS” as an appropriate term to refer to the Kap121p-specific NLS.

Conflict of interest

None.

Acknowledgments

We thank Masako Koyama for assistance and discussion. The X-ray diffraction data collection experiments at the beamline BL41XU of SPring-8 were performed with the approval of the Japan Synchrotron Radiation Research Institute (Proposal No. 2011B1083). This work was supported by JSPS/MEXT KAKENHI (25440019) and the Kurata Memorial Hitachi Science and Technology Foundation.

Transparency document

Transparency document related to this article can be found online at http://dx.doi.org/10.1016/j.bbrc.2015.05.060.

References

[1] C. Wurzenberger, D.W. Gerlich, Phosphatases: providing safe passage through mitotic exit, Nat. Rev. Mol. Cell. Biol. 12 (2011) 469–482.
[2] F. Stegmeier, A. Amon, Closing mitosis: the functions of the Cdc14 phosphatase and its regulation, Annu Rev. Genet. 38 (2004) 203–232.
[3] W. Shou, J.H. Seol, A. Shevchenko, C. Baskerville, D. Moazed, Z.W. Chen, J. Jang, A. Shevchenko, H. Charbonneau, R.J. Deshaies, Exit from mitosis is triggered by Tem1-dependent release of the protein phosphatase Cdc14 from nucleolar RENT complex, Cell 97 (1999) 233–244.
[4] R. Visintin, E.S. Hwang, A. Amon, Cfi1 prevents premature exit from mitosis by anchoring Cdc14 phosphatase in the nucleolus, Nature 398 (1999) 818–823.

[5] J. Bembenek, J. Kang, C. Kurischko, B. Li, J.R. Raab, K.D. Belanger, F.C. Luca, H. Yu, Crm1-mediated nuclear export of Cdc14 is required for the completion of cytokinesis in budding yeast, Cell. Cycle 4 (2005) 961–971.
[6] D.A. Mohl, M.J. Huddleston, T.S. Collingwood, R.S. Annan, R.J. Deshaies, Dbf2-Mob1 drives relocalization of protein phosphatase Cdc14 to the cytoplasm during exit from mitosis, J. Cell. Biol. 184 (2009) 527–539.
[7] Y.M. Chook, K.E. Suel, Nuclear import by karyopherin-betas: Recognition and inhibition, Biochim. Biophys. Acta 1813 (2010) 1593–1606.
[8] J. Kobayashi, Y. Matsuura, Structural basis for cell-cycle-dependent nuclear import mediated by the karyopherin Kap121p, J. Mol. Biol. 425 (2013) 1852–1868.
[9] T. Makhnevych, C.P. Lusk, A.M. Anderson, J.D. Aitchison, R.W. Wozniak, Cell cycle regulated transport controlled by alterations in the nuclear pore complex, Cell 115 (2003) 813–823.
[10] Y. Matsuura, M. Stewart, Structural basis for the assembly of a nuclear export complex, Nature 432 (2004) 872–877.
[11] Collaborative Computational Project Number 4, The CCP4 suite: programs for protein crystallography, Acta Crystallogr. D Biol. Crystallogr. 50 (1994) 760–763.
[12] A. Vagin, A. Teplyakov, Molecular replacement with MOLREP, Acta Crystallogr. D Biol. Crystallogr. 66 (2010) 22–25.
[13] P. Emsley, K. Cowtan, Coot: model-building tools for molecular graphics, Acta Crystallogr. D Biol. Crystallogr. 60 (2004) 2126–2132.
[14] G.N. Murshudov, P. Skubak, A.A. Lebedev, N.S. Pannu, R.A. Steiner, R.A. Nicholls, M.D. Winn, F. Long, A.A. Vagin, REFMAC5 for the refinement of macromolecular crystal structures, Acta Crystallogr. D Biol. Crystallogr. 67 (2011) 355–367.
[15] P.D. Adams, P.V. Afonine, G. Bunkoczi, V.B. Chen, I.W. Davis, N. Echols, J.J. Headd, L.W. Hung, G.J. Kapral, R.W. Grosse-Kunstleve, A.J. McCoy, N.W. Moriarty, R. Oeffner, R.J. Read, D.C. Richardson, J.S. Richardson, T.C. Terwilliger, P.H. Zwart, PHENIX: a comprehensive Python-based system for macromolecular structure solution, Acta Crystallogr. D Biol. Crystallogr. 66 (2010) 213–221.
[16] J. Painter, E.A. Merritt, Optimal description of a protein structure in terms of multiple groups undergoing TLS motion, Acta Crystallogr. D Biol. Crystallogr. 62 (2006) 439–450.
[17] V.B. Chen, W.B. Arendall 3rd, J.J. Headd, D.A. Keedy, R.M. Immormino, G.J. Kapral, L.W. Murray, J.S. Richardson, D.C. Richardson, MolProbity: all-atom structure validation for macromolecular crystallography, Acta Crystallogr. D Biol. Crystallogr. 66 (2010) 12–21.